Disulfide-directed multicyclic peptides for chimeric antigen receptors targeting solid tumors

Xiaoting Meng,[1,2] Keke Fu,[1] Yawei Liu,[1] Yuan Liu,[3] Joe Z. Zhang,[3] Xi Kang,[4]* Chuanliu Wu,[5]* Yu-Hsuan Tsai[1]*

[1] Institute of Molecular Physiology, Shenzhen Bay Laboratory, Shenzhen, China
[2] Division of Life Sciences and Medicine, University of Science and Technology of China, Hefei, China.
[3] Institute of Neurological and Psychiatric Disorders, Shenzhen Bay Laboratory, Shenzhen, China
[4] Translational Innovation Center, Shenzhen Bay Laboratory, Shenzhen, China
[5] Department of Chemistry, College of Chemistry and Chemical Engineering, The Ministry of Education Key Laboratory of Spectrochemical Analysis and Instrumentation, State Key Laboratory of Physical Chemistry of Solid Surfaces, Xiamen University, Xiamen, China
*Correspondence authors: kangxi@szbl.ac.cn; chlwu@xmu.edu.cn; tsai.y-h@outlook.com

Abstract

The clinical application of chimeric antigen receptor (CAR) T cell therapy in solid tumors remains limited due to significant safety concerns, particularly “on-target, off-tumor” toxicity and cytokine release syndrome (CRS). Here, we describe a class of CARs that employ disulfide-directed multicyclic peptides (DDMPs) as compact antigen-recognition domains targeting the tumor-associated antigens HER2 and TROP2. DDMP-based CAR T cells exhibited antigen density-dependent cytotoxicity in vitro and in vivo, efficiently eliminating cells with high antigen expression while sparing cells with low antigen levels, thereby mitigating on-target, off-tumor toxicity. In addition, DDMP-based CAR T cells secreted markedly lower levels of pro-inflammatory cytokines upon targeted killing, reducing the CRS risk. Mechanistic analyses revealed that this favorable combination of restrained cytokine release and density-gated killing is associated with distinct T cell signaling pathway engagement and reduced cell avidity relative to conventional single-chain variable fragment (scFv)-based CAR T cells. Collectively, these findings establish DDMP-based CARs as a promising framework for engineering safer, yet efficacious, CAR T therapies for solid tumors.

Introduction

Cancers are a major global health burden and unmet clinical need. Recently, chimeric antigen receptor (CAR) T cell therapy (**Fig. 1a**) has shown promising results in hematological malignancies.[1] The conventional CAR T manufacturing process involves genetically modifying T cells of the patient to express CARs, which contain antigen recognition, transmembrane, costimulatory, and signaling domains (**Fig. 1b**). The antigen recognition domains are normally single-chain variable fragment (scFv) molecules derived from antibodies targeting specific tumor-associated antigens (TAAs). Upon antigen binding, signal transduction is induced, and the CAR T cells are activated to exhibit tumor-specific killing. Although CAR T therapy has been successful for some hematologic cancers, its efficacy in solid tumors is still limited.[2]

A significant obstacle to CAR T therapy for solid tumors is "on-target, off-tumor" toxicity (**Fig. 1a**), which arises due to the expression of TAAs in both tumor and normal tissues. [3] Unlike hematological CAR T therapies targeting B-cell specific CD19 or BCMA, which do not pose lethal risks to humans upon B-cell depletion,[4] CAR T cells targeting TAAs in solid tumors can inadvertently damage vital healthy tissues, resulting in severe toxicity. For example, a clinical trial of HER2-CAR T resulted in fatal pulmonary toxicity and patient death due to recognition of HER2 expressed in lung tissue.[5]

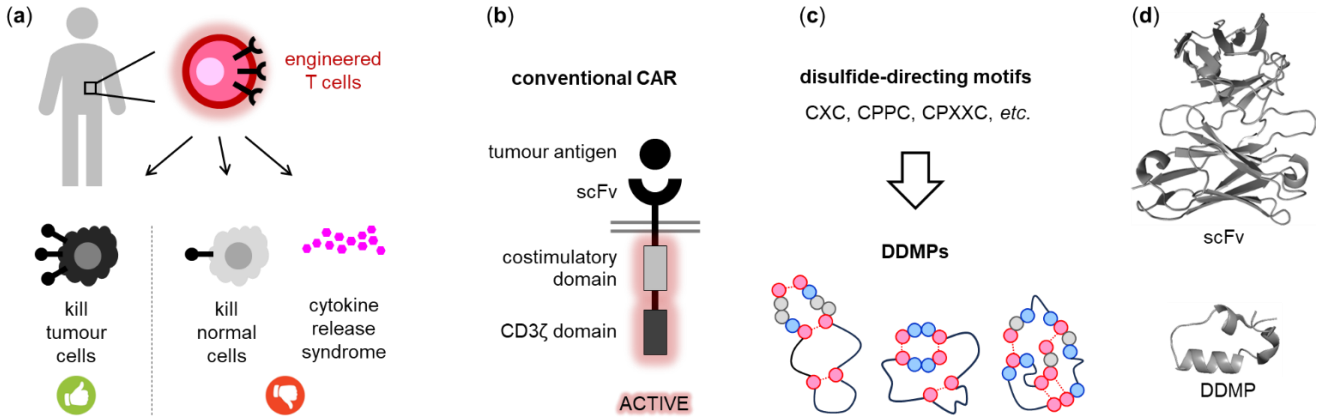

Figure 1. Development of DDMP-based CARs. (a) Schematic of autologous CAR T therapy, highlighting potential on-target, off-tumor toxicity caused by CAR T cells attacking normal cells expressing low levels of the target TAA. Cytokine release syndrome (CRS), a major adverse effect, results from excessive cytokine secretion upon CAR T activation. (b) Structure of conventional CARs, featuring an extracellular scFv domain for antigen recognition. (c) Common disulfide-directing motifs used in constructing DDMPs, including CXC, CPPC, and CPXXC, which preferentially form two disulfide bonds with matching motifs. (d) Ribbon diagrams comparing the size of a typical scFv and a DDMP (PDB: 7YRW) at identical scale.

Furthermore, cytokine release syndrome (CRS) is another common adverse effect of CAR T therapy. This potentially life-threatening condition is triggered by rapid activation and proliferation of CAR T cells, which release large amounts of pro-inflammatory cytokines such as GM-CSF, IFNγ, and TNFα.[6] These cytokines, in turn, activate macrophages and other immune cells. Among the mediators, IL6 produced by activated macrophages acts as a central amplifier of systemic inflammation, driving fever, hypotension, and, in severe cases, multi-organ failure.[7] Continuous monitoring of IL6 levels is therefore an integral part of CRS management. Nevertheless, CRS remains one of the most critical toxicities associated with CAR T-cell therapy, with severe cases occurring in up to 47% of patients,[7] and its treatment continues to impose a substantial burden on clinical resources.

To address these safety concerns, different strategies have been developed. One approach is to tune CAR affinity for the target antigen from very high (e.g., K_D < 1 nM) to a more moderate range (e.g., K_D = 10 – 100 nM), thereby improving discrimination between tumor cells with high antigen density and normal cells with physiological expression.[8-10] This concept is intuitively straightforward, and a recent analysis correlated moderate affinity combined with fast on/off kinetics with improved clinical responses to CAR T therapy in solid tumors.[11] In contrast, attenuating cytokine secretion while preserving cytotoxicity is more challenging, as both are direct consequences of CAR T activation and there is not yet a clear, generalizable relationship between individual CAR design elements and these functional readouts.[12] As a result, extensive engineering is required, with no guarantee of success. Other safety-improvement strategies, including on-switch CARs, inhibitory CARs, suicide genes, and synthetic Notch receptors,[13] can add layers of control over CAR T activity but require additional genetic modules, complicating manufacturing and quality control. More recently, effective CAR T cells based on alternative antigen-recognition modules, rather than conventional scFvs, have demonstrated that the binding domain can be exploited to fine-tune CAR T function.[14-16]

Peptides are promising antigen recognition modules due to their small molecular size, high structural diversity, and wide design flexibility. Multicyclic peptides, stabilized through covalent bonds, are particularly appealing.[17] These peptides possess enhanced structural rigidity and metabolic stability compared to their linear and monocyclic counterparts. They can also bind challenging targets with antibody-like specificity and affinity.[18] Disulfide-directed multicyclic peptides (DDMPs) represent a novel class of such peptides, engineered using motifs that promote specific disulfide pairing (e.g., CXC, CPPC or CPXXC motif, where C = Cys, P = Pro, X = any; **Fig. 1c** and **1d**)[19] or enhance folding efficiency.[20] DDMPs enable the creation of diverse, structurally stable peptide libraries that can be subjected to directed evolution via mRNA, phage, or yeast display technologies.[21-23] These peptides have demonstrated potent protein-binding capabilities and are tolerant to extensive sequence manipulations, making them suitable for ligand and drug discovery.

Here, we describe the design and characterization of three DDMP-based CARs targeting the clinically relevant TAAs HER2 and TROP2, which are frequently overexpressed across solid tumors. Across multiple in vitro and in vivo models, DDMP-based CAR T cells retained robust antitumor activity while displaying pronounced antigen density-dependent cytotoxicity, efficiently clearing antigen-overexpressing cells but sparing those with low antigen levels, thereby attenuating on-target, off-tumor toxicity. Moreover, DDMP-CAR T cells produced substantially lower amounts of pro-inflammatory cytokines upon target engagement, consistent with a reduced propensity for CRS. Mechanistic studies further revealed that these functional advantages are associated with altered T cell signaling and cell avidity, distinguishing DDMPs from conventional scFv scaffolds in terms of downstream programming. Collectively, our work illustrates how chemical innovation in protein binder design can drive advances in biomedical applications. Specifically, we establish DDMPs as a compact and structurally robust extracellular recognition module for CAR engineering and highlight DDMP-based CARs as a promising platform for developing safer yet effective T cell therapies against solid tumors.

Results

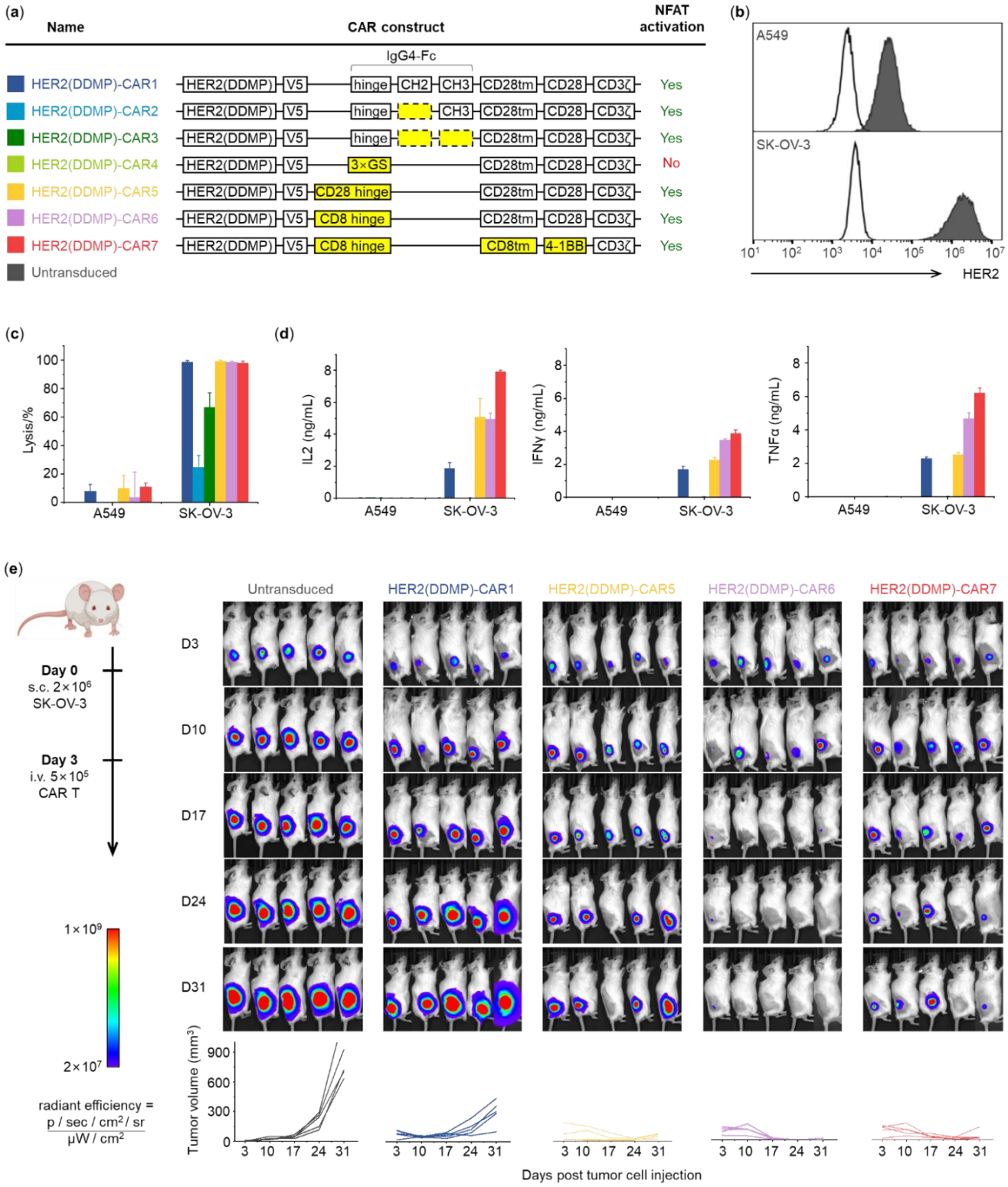

Figure 2. Construction of an effective, HER2-targeting DDMP-CAR. (a) Diagram of HER2(DDMP)-CAR variants and their functional analysis via NFAT activation in Jurkat-NFAT cells. Differences from CAR1 are highlighted in yellow. IgG4-Fc includes L235E and N297Q mutations to minimize FcγR binding.[24] For functional analysis, the candidate construct was expressed in Jurkat-NFAT reporter cells, which were incubated with SK-OV-3 target cells overexpressing the cognate antigen HER2. Activation was quantified via expression of the NFAT-dependent GFP reporter gene. CAR expression was assessed via the V5 tag (**Fig. S2a**). Representative NFAT activation histograms by flow cytometry are shown in **Fig. S2b**. (b) Target antigen profiling. Flow cytometry histograms of cell-surface HER2 on A549 and SK-OV-3 stained with α-HER2 antibody. X-axis: HER2 fluorescence intensity; Y-axis: cell count. Quantitative HER2 levels for all cell lines used in evaluating HER2-CAR T (including A549 and SK-OV-3) are summarized in **Fig. S1**. (c) In vitro cytotoxicity. Killing of A549 or SK-OV-3 cells by CAR T cells. Effector and target cells were co-cultured at the ratio of 1:20 for four days, followed by flow cytometry analysis. See **Fig. S3** for representative histograms. CAR

expression in T cells ($CD3^+$) is shown in **Fig. S3a**. Gating strategy to distinguish tumor cells (GFP^+) and T cells ($CD3^+$) is shown in **Fig. S3b**. (d) Cytokine release. IL2, IFNγ, and TNFα in supernatants after 24-hour co-culture of CAR T cells with A549 or SK-OV-3 at the ratio of 2:1, quantified by ELISA. (e) In vivo efficacy of HER2(DDMP)-CAR T cells in a SK-OV-3-luc xenograft model. Representative bioluminescence images and caliper-measured tumor volume are shown. An illustration of the experimental design timeline is shown on the left. Female NCG mice were subcutaneously (s.c.) engrafted with SK-OV-3-luc-GFP cells. Maximum and minimum bioluminescence values are shown at the top and bottom of the scale bars. Individual mice data of tumor signal, tumor volume and body weight are shown in **Fig. S4**.

Construction of multicyclic peptide-based, HER2-targeted CAR

We previously identified a DDMP binder to human HER2 extracellular domain.[25] This HER2(DDMP) displays fast on/off binding kinetics with moderate affinity (K_D ~ 60 nM), which was proposed to be a desirable characteristic for CAR T against solid tumors.[11] We first designed seven HER2(DDMP)-CAR constructs based on the literature.[16, 26-28] These constructs share a conserved antigen recognition motif (i.e., the HER2-binding DDMP), a V5 tag for quantifying CAR expression and cytosolic CD3ζ sequence for signaling (**Fig. 2a**). The constructs differ in the linker (full-length or truncated IgG4-Fc, CD8 hinge, CD28 hinge or GSGSGS hexapeptide), transmembrane domain (derived from CD8 or CD28), or costimulatory domain (derived from CD28 or 4-1BB).

We screened the CAR function in human $CD4^+$ Jurkat T cell line. Cells were engineered with NFAT response elements controlling GFP expression, enabling T cell activation to be visualized via fluorescence.[29] The Jurkat-NFAT reporter cells were transduced with lentivirus encoding different CAR constructs. Cells were then incubated with SK-OV-3, an ovarian cancer cell line overexpressing HER2 (**Fig. 2b** and **S1**). All HER2(DDMP)-CARs, except CAR4 with a GSGSGS hexapeptide linker, could activate NFAT signaling upon co-culture with SK-OV-3 cells yielding green fluorescent Jurkat-NFAT reporter cells, indicating functionality of the corresponding constructs (**Fig. 2a** and **S2**). We then evaluated the *in vitro* tumor killing by co-culturing CAR T cell variants with tumor cells expressing low or high density of HER2 at an effector-to-tumor (E:T) ratio of 1:20 in long-term assays.[28] Human T cells isolated from healthy donors were transduced with lentiviruses encoding HER2(DDMP)-CAR (**Fig. S3a)**. The variants with the linker sequence of full-length IgG4-Fc (CAR1), CD28 hinge (CAR5) or CD8 hinge (CAR6 & CAR7) demonstrated potent and comparable cytotoxicity against $HER2^{high}$ SK-OV-3 cells but not against $HER2^{low}$ A549 cells (**Fig. 2c** and **S3b**). The HER2-specific cytotoxicity was evident by both diminishing tumor cell and expanding T cell populations. These CAR T cells also produced cytokines IL2, IFNγ and TNFα upon co-culture with SK-OV-3 (**Fig. 2d**). The level of cytokines broadly follows the order of CAR7 (CD8h-BBz) > CAR6 (CD8h-28z) > CAR5 (CD28h-28z) > CAR1 (IgG4-Fc-28z). On the other hand, negligible cytokines were secreted by CAR2 and CAR3 lacking *in vitro* cytotoxicity against $HER2^{high}$ SK-OV-3 cells. In addition, no cytokine was detected for any CAR T constructs co-cultured with $HER2^{low}$ A549 cells.

We next investigated the *in vivo* therapeutic activity of these HER2(DDMP)-CAR variants. Female immunodeficient NCG mice were subcutaneously engrafted with 2×10^6 SK-OV-3 cells. Three days later, the mice were subjected to adoptive transfer of 5×10^5 CAR T cells by intravenous injection (**Fig. 2e**). Untransduced T cells were used as the negative control, and we found that T cells expressing HER2(DDMP)-CAR5/6/7 effectively controlled tumor growth, as evidenced by diminished signal in bioluminescence images and reduced caliper-measured tumor volume in the plots (**Fig. 2e** and **S4**). Based on the residual luminescence and tumor volume, HER2(DDMP)-CAR6 demonstrated the highest *in vivo* efficacy and was chosen for subsequent comparison with conventional CAR based on single-chain variable fragment (scFv) for antigen recognition.

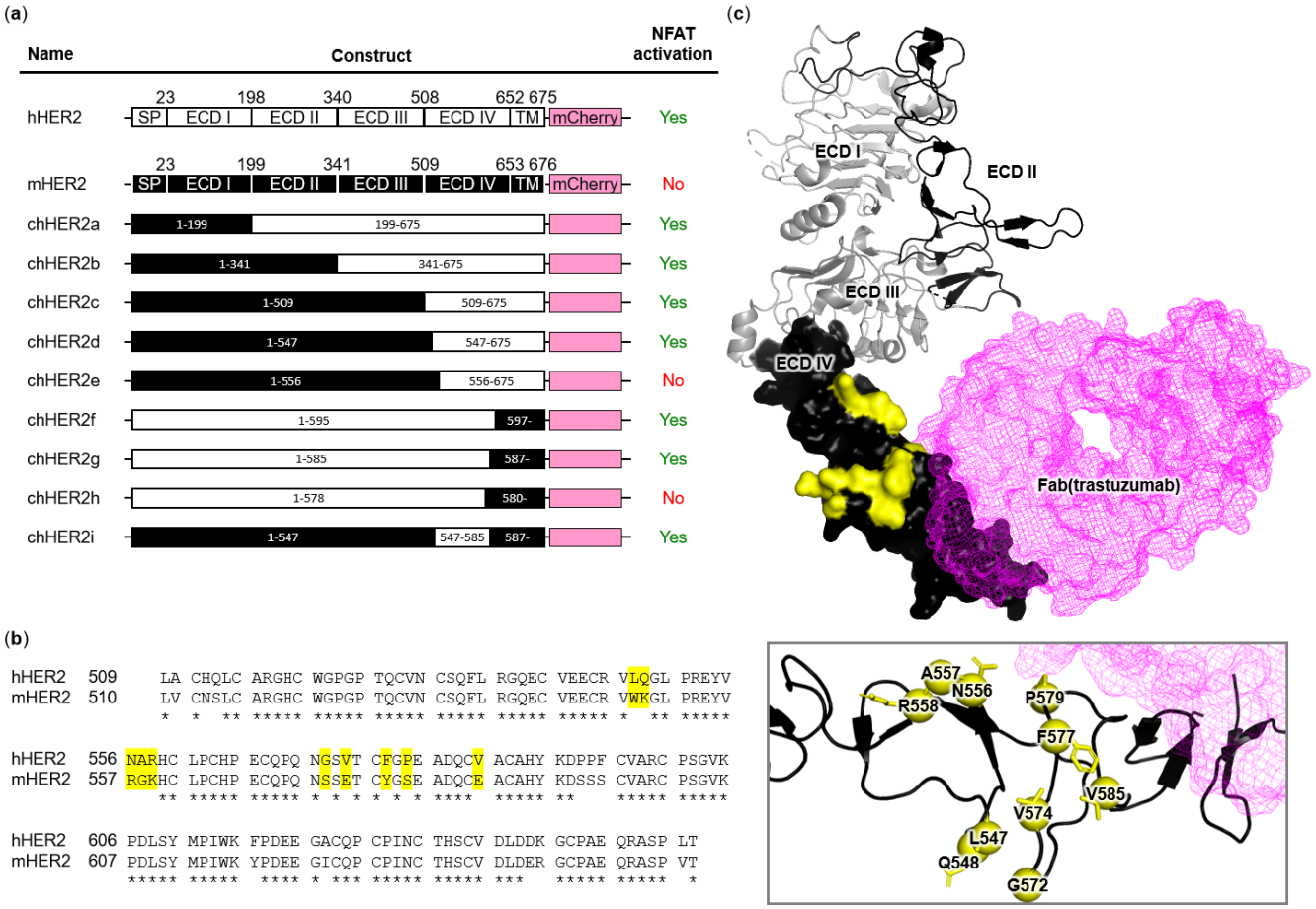

Figure 3. Elucidation of the HER2(DDMP) binding epitope. (a) Schematic presentation of different HER2 constructs and their ability to activate HER2(DDMP)-CAR Jurkat-NFAT cells. Jurkat-NFAT cells were transduced with a lentivirus encoding HER2(DDMP)-CAR1 and then incubated with HEK293T cells overexpressing different HER2 variants. Activation was quantified via expression of a NFAT-dependent GFP reporter gene. See **Fig. S5** for representative histograms by flow cytometry. (b) Sequence alignment of ECD IV between human HER2 (509-652, UniProt: P04626) and mouse HER2 (510-653, UniProt: P70424). Residues potentially critical for HER2(DDMP) binding are highlighted in yellow. (c) Structure of human HER2 ECD in complex with trastuzumab Fab (PDB: 1N8Z). ECD I-III are shown in "cartoon" presentation, and ECD IV is shown in "surface" presentation. Residues potentially critical for HER2(DDMP) binding are shown in yellow and labeled in the box below with side chains in "stick" presentation. Trastuzumab Fab is colored in pink and shown in "mesh" presentation. hHER2: human HER2; mHER2: mouse HER2; chHER2: chimeric HER2; SP: signal peptide; ECD: extracellular domain; TM: transmembrane domain.

Elucidation of the multicyclic peptide binding epitope on HER2

Conventional scFv-based CAR could elicit different in vitro and in vivo activities depending on their binding epitope of the target antigen.[26, 30] To compare the functional differences between DDMP- and scFv-based CARs, it would be ideal to use binders to an identical epitope. Since the epitope of HER2(DDMP) was unknown, we first elucidated its binding site. We found that Jurkat-NFAT cells expressing HER2(DDMP)-CAR could be activated upon incubation with HEK293T cells overexpressing human HER2 (hHER2) but not mouse HER2 (mHER2, **Fig. 3a** and **S5**), indicating species-specific binding. Since extracellular domain (ECD) of HER2 can be divided into four subdomains (I-IV),[31] we then generated chimeric HER2 constructs containing either mHER2 ECD I (chHER2a), mHER2 ECD I-II (chHER2b) or mHER2 ECD I-III (chHER2c), followed by hHER2. We found HEK293T overexpressing any of these constructs could activate HER2(DDMP)-CAR Jurkat-NFAT cells, indicating binding of HER2(DDMP) to hHER2 ECD IV. Further analysis indicated the involvement of hHER2 L547/Q548 (chHER2d-e) and P579/V585 (chHER2f-h) in interaction with HER2(DDMP). Indeed, chHER2 containing hHER2(547-585) was able to activate HER2(DDMP)-CAR Jurkat-NFAT cells. Within this sequence, 10 amino acid residues are different between hHER2 and mHER2 (**Fig. 3b**), and this region is proximal to the trastuzumab binding site (**Fig. 3c**).

Attempts to generate a model of hHER2 and HER2(DDMP) using AlphaFold2 was unsuccessful as none of the generated models showed the involvement of L547/Q548/P579/V585 to HER2(DDMP).[32-33]

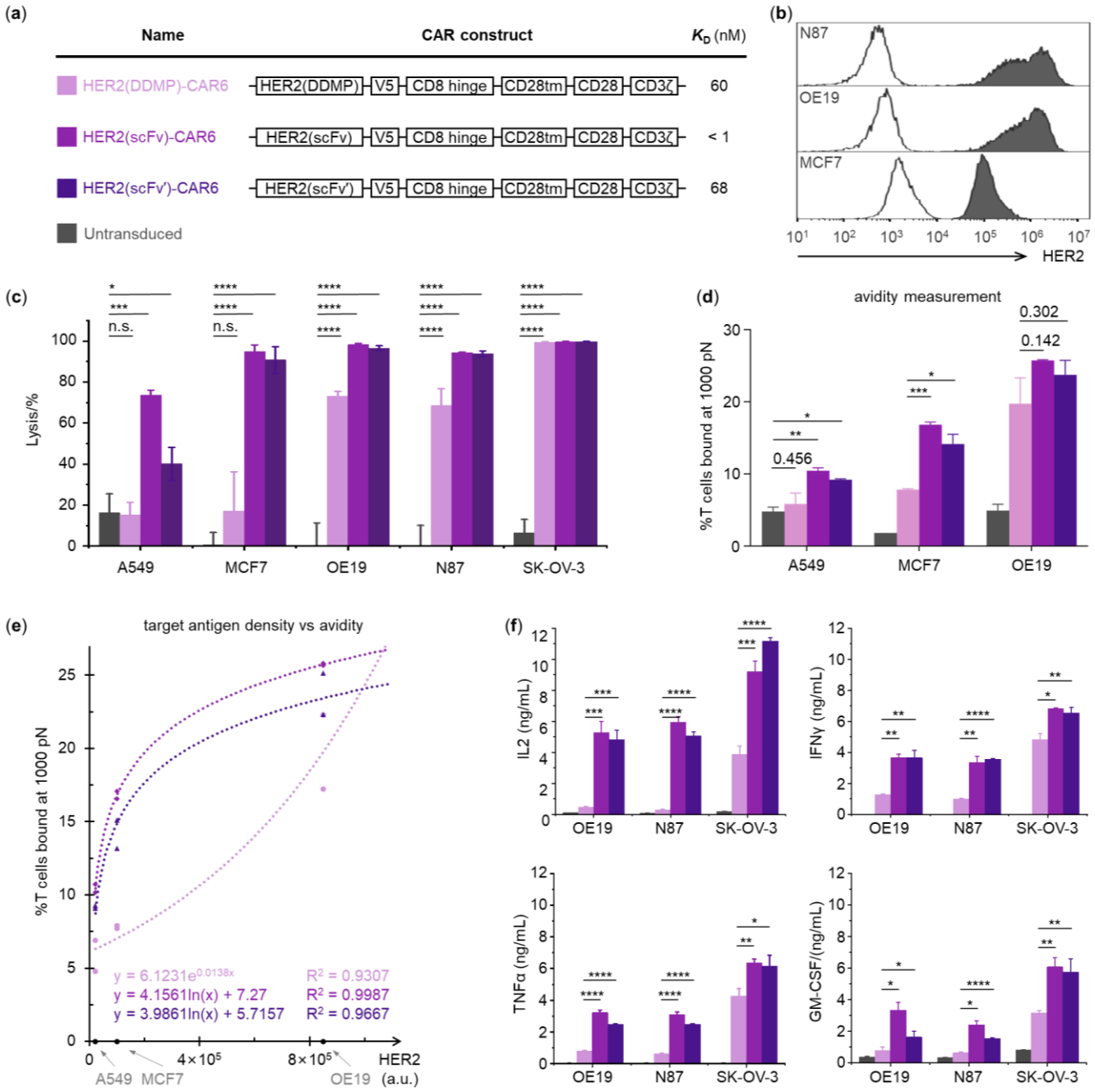

Figure 4. In vitro evaluation of DDMP- and scFv-based HER2-CAR constructs. (a) CAR constructs and affinities. Domain architecture of the HER2-CAR constructs and their equilibrium dissociation constants (K_D) for human HER2. The HER2(DDMP) construct (moderate affinity) is compared with two trastuzumab-derived scFv CARs (high-affinity scFv and moderate-affinity scFv′). (b) Target antigen profiling. Flow cytometry histograms of cell-surface HER2 on MCF7, OE19, and N87 cells stained with α-HER2 antibody. X-axis: HER2 fluorescence intensity; Y-axis: cell count. Quantitative HER2 levels for all cell lines used in evaluating HER2-CAR T (including A549 and SK-OV-3) are summarized in **Fig. S1**. (c) In vitro cytotoxicity. Killing of A549, MCF7, OE19, N87, and SK-OV-3 cells by CAR T cells. Effector and target cells were co-cultured at the ratio of 1:20 for four days, followed by flow cytometry analysis. See **Fig. S6** for representative histograms. (d) Cell avidity by z-Movi as fractional binding at 1000 pN. Adhesion strength of T cells to A549, MCF7 or OE19 monolayers was quantified using z-Movi acoustic force spectroscopy. Full binding profiles are shown in **Fig. S7**. (e) Target antigen density versus avidity.[34] HER2 levels (x-axis) are represented by the median fluorescence intensity from flow cytometry data (see **Fig. S1**). Trendlines represent the best-fit model for each construct (exponential for DDMP, logarithmic for scFv). (f) Cytokine release. IL2, IFNγ, TNFα, and GM-CSF in supernatants after 18-hour co-culture of CAR T cells with OE19, N87, or SK-OV-3 at the ratio of 2:1, quantified by ELISA.

Trastuzumab, which originated from the murine monoclonal antibody 4D5, is widely used in HER2-targeted therapies.[35] This antibody binds to human HER2 ECD IV [36] and is in clinical use for treatment of HER2-positive breast or gastric cancer. The scFv of trastuzumab has also been used to construct HER2-targeted CAR by different groups.[37-41] Since both HER2(DDMP) and trastuzumab bind to hHER2 ECD IV, we then evaluated the functional difference between HER2(DDMP)-CAR and HER2(scFv)-CAR based on trastuzumab.

HER2(DDMP)-CAR T cells exhibit reduced on-target, off-tumor cytotoxicity and cytokine secretion

For comparative studies, we constructed HER2(scFv)-CAR6, which replaces the HER2-targeting multicyclic peptide in HER2(DDMP)-CAR6 with trastuzumab scFv. Since trastuzumab scFv binds much tighter to hHER2 (K_D < 1 nM),[37] we also included a scFv variant with comparable affinity (K_D = 68 nM)[42] to HER2(DDMP) to construct HER2(scFv′)-CAR6 (**Fig. 4a**).

We first evaluated the in vitro cytotoxicity of the three CAR variants. All constructs displayed potent and comparable killing against HER2^{high} OE19, N87 and SK-OV-3 cells (**Fig. 4b** and **S6**), which are derived from esophageal, gastric, and ovarian cancers, respectively. However, the two scFv constructs also showed statistically significant cytotoxicity against HER2^{low} A549 and HER2^{moderate} MCF7 cells, in contrast to T cells expressing HER2(DDMP)-CAR6. Activity against HER2^{low} A549 or HER2^{moderate} MCF7 cells was also evident based on CAR T proliferation, which was most pronounced for the high-affinity HER2(scFv)-CAR6.

To investigate the basis of these differences, we measured the avidity of CAR T cells toward targets expressing varying levels of HER2. Avidity has emerged as a key biomarker of CAR T efficacy, often correlating more strongly with therapeutic function than conventional in vitro assays.[43] Overall, avidity trends mirrored cytotoxicity profiles (**Fig. 4d** and **S7**). Notably, against HER2^{low} A549 cells, HER2(DDMP)-CAR6 T cells exhibited no statistically significant increase in avidity compared to untransduced T cells, whereas both HER2(scFv)-CAR6 and HER2(scFv′)-CAR6 T cells showed significantly higher avidity. In contrast, against HER2^{high} OE19 cells, all CAR constructs demonstrated markedly elevated avidity relative to untransduced T cells, with no statistically significant differences between the CAR variants. These data indicate that HER2(DDMP)-CAR6 follows a threshold-like, “cooperative” avidity profile (**Fig. 4e**): it shows minimal binding to cells with low or moderate HER2 expression (A549 and MCF7), but avidity increases sharply once HER2 density exceeds a certain level, as in OE19. In this regime, stable CAR–target engagement is favored only when antigen density is sufficiently high to support multivalent or sustained interactions, thereby promoting selective recognition of highly HER2-positive tumor cells while limiting engagement of normal cells with low HER2 expression. In contrast, HER2(scFv)-CAR6 and HER2(scFv′)-CAR6 exhibit a more gradual, “logarithmic” avidity curve, with substantial increases in binding already evident at modest elevations in HER2 expression, enhancing cytotoxic potential but reducing antigen-density selectivity. Together, these findings support avidity as a key mechanistic determinant of the density-gated cytotoxicity observed for DDMP-based HER2-CAR T cells.

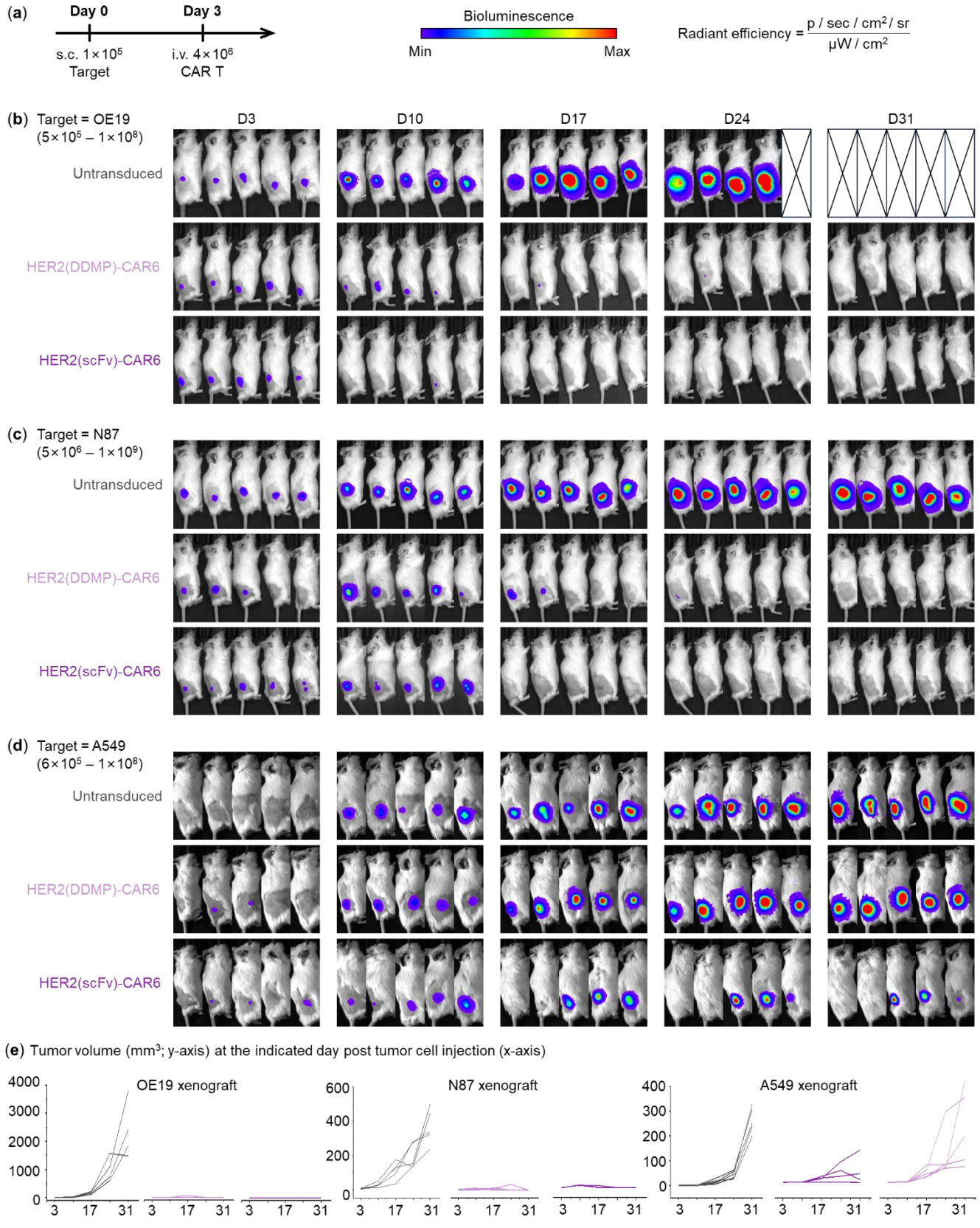

Figure 5. In vivo evaluation of DDMP- and scFv-based HER2-CAR T cells. (a) Study schematics. Timeline of xenograft establishment, and CAR T cell infusion. (b-d) Subcutaneous xenograft models. Male immunodeficient NCG mice were subcutaneously (s.c.) engrafted with 1×10^5 OE19-luc-GFP (b), N87-luc-GFP (c) or A549-luc-GFP (d) cells. On day 3 (D3), mice received 4×10^6 CAR T cells or untransduced T cells (negative control) via intravenous (i.v.) infusion. Representative bioluminescence images are shown with intensity scales set to 5×10^5 – 1×10^8 for (b), 5×10^6 – 1×10^9 for (c), and 6×10^5 – 1×10^8 for (d). (e) Caliper-measured tumor volume of individual mice in (b-d). Corresponding quantitative tumor signal (total flux) and body weight for individual mice are shown in **Figs. S9-S11**.

We next assessed cytokine release after co-culture with HER2^{high} OE19, N87 and SK-OV-3 cells. Interestingly, HER2(DDMP)-CAR6 T cells secreted substantially lower levels of IL2, IFNγ, TNFα and GM-CSF than T cells expressing either the high-affinity HER2(scFv)-CAR6 or the comparable affinity HER2(scFv′)-CAR6 (**Fig. 4f**). This reduction was consistent across different E:T ratios (E = effector, i.e., CAR T cells; T = target, i.e., OE19 in this experiment) and occurred despite comparable in vitro cytotoxicity among the three constructs (**Fig. S8**), indicating that the DDMP-CAR preserves tumor killing while attenuating pro-inflammatory cytokine production. Among these cytokines, GM-CSF drives granulocyte and macrophage proliferation and activation,[44-45] whereas IFNγ and TNFα further promote macrophage activation.[46-47] In the setting of CAR T therapy, IL6 released by activated macrophages is the key driver of CRS-associated toxicities.[6] Thus, lowering upstream cytokines such as GM-CSF, IFNγ and TNFα is expected to limit macrophage activation and mitigate CRS risk at its source.

For in vivo efficacy (**Fig. 5**), HER2(DDMP)-CAR6 achieved tumor control comparable to the high-affinity HER2(scFv)-CAR6 against HER2^{high} OE19 (**Fig. 5b** and **S9**) and N87 (**Fig. 5c** and **S10**) xenografts, as evidenced by reductions in both bioluminescent signal and caliper-measured tumor volume. In contrast, HER2(scFv)-CAR6 also markedly suppressed HER2^{low} A549 tumors, whereas HER2(DDMP)-CAR6 spared these cells (**Fig. 5d** and **S11**). Together, these findings support a superior safety profile for HER2(DDMP) in CAR design, preserving antitumor activity at high antigen density while minimizing on-target, off-tumor activity and the attendant risk of cytokine-driven toxicities.

TROP2(DDMP)-CAR T cells induce less cytokine secretion

To assess the broader applicability of the DDMP-based CAR strategy, we turned to trophoblast cell-surface antigen 2 (TROP2), another frequently overexpressed TAA.[48-49] Our prior investigation showed that TROP2(DDMP*)-CAR6 T cells (**Fig. 6a**) selectively lysed TROP2-overexpressing cells while minimizing cytokine secretion and sparing cells with low TROP2 expression.[20] To further dissect scaffold effects, we selected another DDMP binder with a distinct backbone and affinity (Table 1) to generate TROP2(DDMP)-CAR7, and constructed an affinity-matched TROP2(scFv)-CAR7 based on the clinically approved TROP2-specific antibody drug conjugate sacituzumab govitecan.

In vitro cytotoxicity was assessed by co-culturing CAR T cells (**Fig. S12**) with parental A549 or A549-TROP2 (engineered to overexpress TROP2) at E:T = 1:5 in long-term assays (**Fig. 6b**). All constructs mediated robust and comparable killing of A549-TROP2, with negligible activity against TROP2-negative A549 cells (**Fig. 6c** and **S13**). While both TROP2(DDMP)-CAR7 and TROP2(scFv)-CAR7 elicited cytokines only upon engagement with A549-TROP2, TROP2(DDMP)-CAR7 secreted substantially lower levels of IL2, IFNγ, TNFα, and GM-CSF than the scFv counterpart (**Fig. 6d**). Importantly, all constructs showed comparable in vivo antitumor efficacy against subcutaneous A549-TROP2 xenografts (**Fig. 6e** and **Fig. S14**), indicating a scaffold and target-independent DDMP-CAR phenotype that preserves potency while attenuating pro-inflammatory cytokine production.

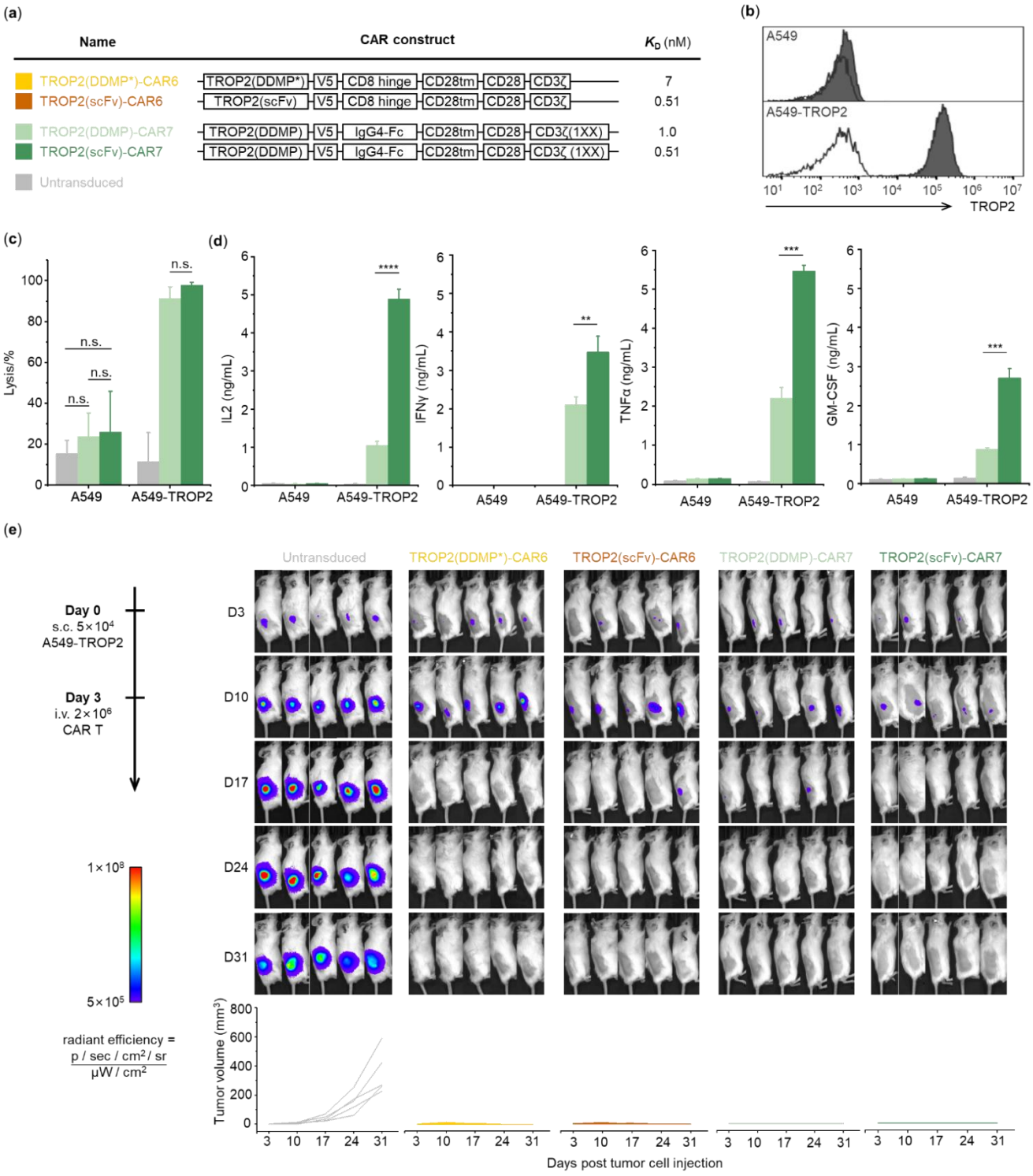

Figure 6. Comparison of DDMP- and scFv-based TROP2-CAR. (a) CAR constructs and affinities. Domain architecture of the TROP2-CAR constructs and their equilibrium dissociation constants (K_D) for human TROP2. (b) Target antigen profiling. Flow cytometry histograms of cell-surface TROP2 on A549-luc-GFP and A549-TROP2-luc-GFP stained with α-TROP2 antibody. X-axis: TROP2 fluorescence intensity; Y-axis: cell count. (c) In vitro cytotoxicity. Killing of TROP2^{low} A549-luc-GFP or TROP2^{high} A549-TROP2-luc-GFP by CAR T cells. Effector and target cells were co-cultured at the ratio of 1:5 for four days, followed by flow cytometry for quantitative analysis. See **Fig. S13** for representative histograms. (d) Cytokine release. IL2, IFNγ, TNFα, and GM-CSF in supernatants after 18-hour co-culture of CAR T cells with TROP2^{low} A549-luc-GFP or TROP2^{high} A549-TROP2-luc-GFP at the ratio of 2:1 for 18 h, quantified by ELISA. (e) In vivo efficacy of TROP2-CAR T cells in an A549-TROP2-luc-GFP xenograft model. Representative bioluminescence images and caliper-measured tumor volume are shown. An illustration of the experimental design timeline is shown on the top. Male NCG mice were subcutaneously (s.c.) engrafted with the tumor cells. Individual mice data of tumor signal, tumor volume and body weight are shown in **Fig. S14**.

Transcriptional differences between DDMP- and scFv-based CARs

To gain a more comprehensive view of the phenotypic differences between DDMP- and scFv-based CAR T cells, we performed bulk RNA-seq on CAR T cells prepared from three independent donors (**Fig. 7a**). HER2- and TROP2-CAR T cells were stimulated with OE19 and A549-TROP2 cells, respectively, before mRNA isolation and sequencing. Principal component analysis (PCA) separated CAR T cells from untransduced controls (**Fig. 7b**) and, in pairwise comparisons, further resolved DDMP and scFv cohorts into distinct clusters (**Fig. 7c**). Consistently, the heatmap of the top 100 differentially expressed genes (DEGs) showed a clear distinction between untransduced, DDMP-based CAR, and scFv-based CAR T cells (**Fig. 7d**).

Pathway analysis revealed divergent signaling programs (**Fig. S15**). DDMP-based CAR T cells displayed reduced expression of pro-inflammatory cytokine genes (**Fig. S15c**), in line with their attenuated cytokine secretion (**Fig. 4f** and **6d**), and increased expression of proliferation-associated genes, suggesting enhanced expansion and persistence potential (**Fig. S15d**). They also exhibited unique patterns across gene sets linked to T-cell dysfunction, inhibitory receptors, effector differentiation, and metabolic pathways (**Fig. S15e**). Notably, transcriptional signatures favored a more naïve/memory-like state in DDMP-based CAR T cells, an attribute associated with durable antitumor responses (**Fig. S15e**).

T cell activation engages the NFAT, RAS/MAPK, JNK/c-Jun and NF-κB pathways, all of which contribute to the transcription of cytokine genes. We therefore performed gene set enrichment analysis (GSEA) to assess pathway-level differences between DDMP and scFv cohorts. Among the 50 hallmark gene sets, only “KRAS signaling up” and “TNF signaling via NF-κB” directly relate to T cell activation. Accordingly, we also analyzed NFAT, NF-κB and c-Jun sets from the legacy transcription factor targets (TFT). These sets comprise genes induced by specific pathways or transcription factors. Overall, relative to scFv-based CARs, DDMP-based CARs showed negative enrichment of NFAT, RAS, and NF-κB responsive transcripts, but not c-Jun (**Fig. 7e**). Pairwise comparisons confirmed a consistent and significant reduction in NF-κB responsive transcripts across DDMP constructs. However, KRAS differences reached significance only for HER2(DDMP)-CAR6 and TROP2(DDMP*)-CAR6, and NFAT for TROP2(DDMP*)-CAR6 (**Fig. S16**–**S19**). As expected, both CAR types showed upregulation versus untransduced T cells across these modules, consistent with T cell activation upon antigen encounter. Together, these data indicate that attenuated NF-κB transcriptional output is the predominant driver of the reduced cytokine program in DDMP-CAR T cells, with construct-dependent contributions from KRAS and NFAT pathways.

Overall, the transcriptomic profiles of DDMP-based CAR T cells are characterized by dampened cytokine programs, enhanced proliferative signatures, preservation of memory features, and selective down-modulation of NF-κB responsive transcripts, supporting DDMP as a promising scaffold for engineering safer, equally effective CAR T therapies against solid tumors.

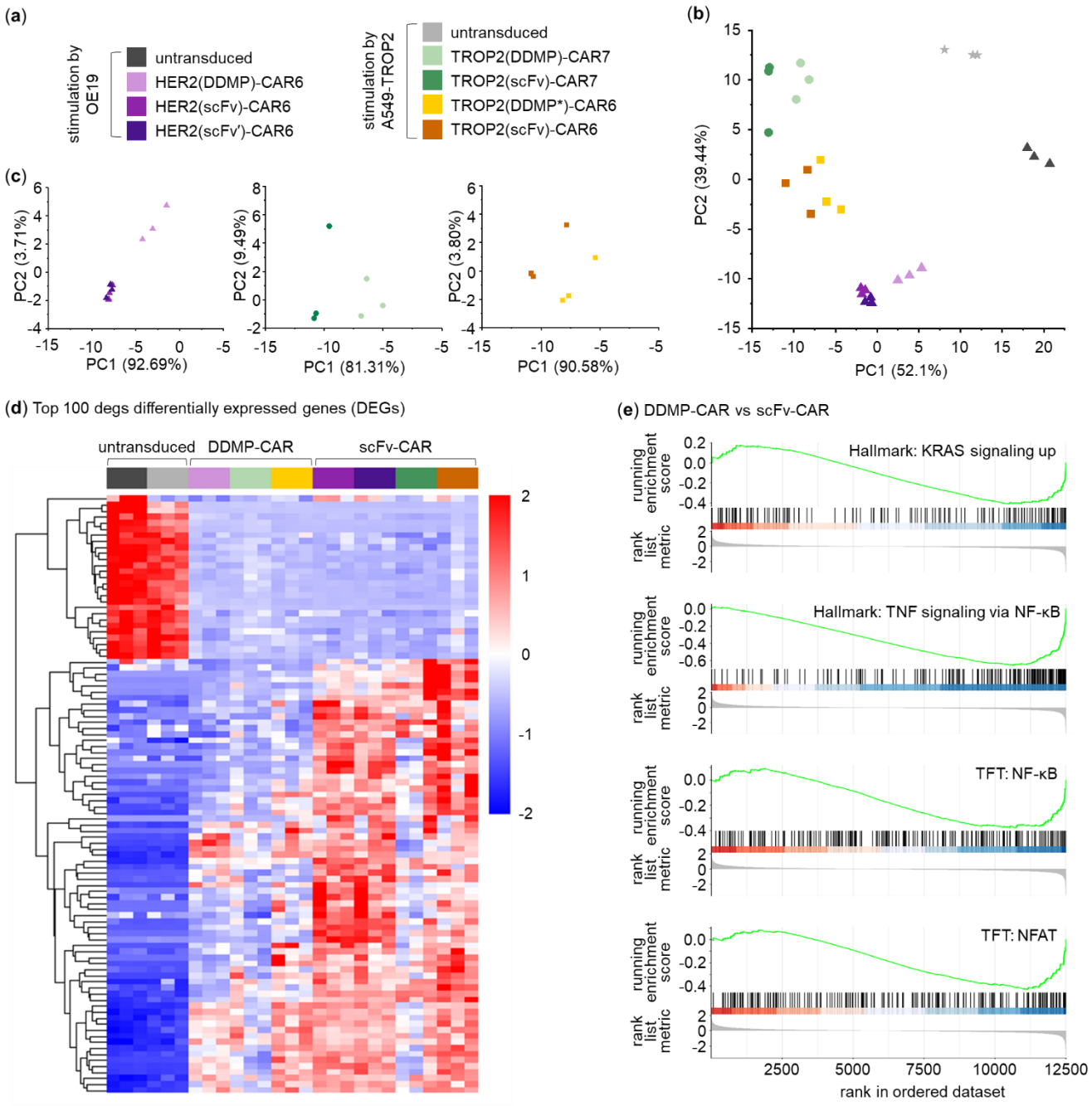

Figure 7. Transcriptomic profiling of DDMP- and scFv-CAR T cells after antigen stimulation. (a) Legend of HER2- and TROP2-targeting CAR constructs used in RNA-seq. Cells were stimulated with OE19 or A549-TROP2 cells for 18 hours at E:T = 2:1. (b-c) Principal component analysis (PCA) of stimulated CAR T cells. (d) Heatmap of top 100 differentially expressed genes (DEGs) of untransduced T cells (left), DDMP-based CAR T cells (middle) and scFv-based CAR T cells (right) after antigen stimulation. (e) Gene set enrichment analysis (GSEA) comparing DDMP- versus scFv-based CAR T cells. Shown are the Hallmark gene sets HALLMARK_KRAS_SIGNALING_UP (genes up-regulated by KRAS activation) and HALLMARK_TNFA_SIGNALING_VIA_NFKB (genes regulated by NF-κB in response to TNF), together with NF-κB and NFAT transcription factor target gene sets from the C3:TFT legacy collection. See **Fig. S16**–**S19** for pairwise comparisons.

Discussion

Considerable safety concerns, notably on-target, off-tumor toxicity and CRS, remain critical barriers to effective CAR T therapy for solid tumors. A generalizable strategy to mitigate both issues concurrently in conventional scFv-based CARs is still lacking.[8-13] In addition, the therapeutic profile of scFv-CARs can be compromised by the intrinsic instability and aggregation propensity of certain scFv sequences.[50-52] Motivated by these challenges and by emerging evidence that alternative antigen-recognition modules can successfully tune CAR function,[14-16] we turned to DDMPs as a chemically distinct and compact class of binding domains for next-generation CAR design.

DDMPs represent a versatile molecular recognition scaffold, in which disulfide-directing motifs promote defined oxidative folding into multicyclic peptides with high sequence adaptability.[19-20] DDMP-based ligands have been developed against multiple cell-surface proteins, including EphA2, FGFR1, HER2, HER3, ROR1, and TROP2.[25, 53-54] Building on this chemical scaffold, we explored three DDMPs, HER2(DDMP), TROP2(DDMP) and TROP2(DDMP*), as CAR antigen-recognition domains. These sequences, identified by phage display, exhibit good in vitro oxidative folding efficiency (i.e., 68%, 46% and 65%, respectively). The presence of chaperones and protein quality control machinery in mammalian cells is expected to further favor the presentation of the correctly folded structure on the cell surface. Structurally, DDMPs exhibit high conformational stability and significant resistance to enzymatic degradation, while their low molecular weight (<5 kDa) minimizes the genetic footprint, leaving additional design space on viral vectors for auxiliary elements, further boosting CAR T efficacy.

Table 1. Binding kinetics and affinity of the antigen-recognition elements used in this study.

	DDMP backbone	k_{on} (10^5 M^{-1} s^{-1})	k_{off} (10^{-4} s^{-1})	K_D (nM)	Ref
HER2(DDMP)	$CPX_2CX_3CX_5CX_7CPX_2C$	6.36	383	60	[25]
HER2(scFv)	not applicable	2.14	1.22	0.52	[42]
HER2(scFv')	not applicable	1.60	154	68	[42]
TROP2(DDMP)	$CPPCX_5CX_5CX_5CPPC$	6.21	6.11	0.98	[55]
TROP2(DDMP*)	$CXPX_3PCXPX_3PCCX_2PCPX_8CXCC$	14.1	99.0	7.0	20
TROP2(scFv)	not applicable	1.02	0.821	0.81	[56]

Kinetic analysis highlights additional advantages of the DDMP scaffold. The three DDMPs used here have distinct backbones (**Table 1**) but share similar association rate constants (k_{on}, ~ 6 – 14 × 10^6 M^{-1} s^{-1}) and differ primarily in dissociation rate (k_{off}, ~ 6 – 400 × 10^{-4} M^{-1} s^{-1}), yielding affinities (K_D = k_{off} / k_{on}) spanning 1 – 60 nM. In all cases, DDMPs exhibit faster association and dissociation than their scFv counterparts. A recent clinical analysis suggests that CAR T cells with moderate affinity and fast on/off kinetics are associated with improved outcomes in solid tumors.[11] Consistent with this, CAR T cells based on the moderate-affinity HER2(DDMP) and TROP2(DDMP*) showed clear density-gated cytotoxicity in vitro, efficiently eliminating antigen-overexpressing targets while largely sparing cells with low antigen expression, in contrast to the broader killing profile of scFv-based CARs. This antigen-density dependence is recapitulated in xenograft models for HER2(DDMP)-CAR (**Fig. 5**). Avidity measurements by z-Movi

provide a mechanistic explanation: HER2(DDMP)-CAR T cells display relatively low functional avidity for $HER2^{low/moderate}$ cells (A549 and MCF7 in **Fig. 4d**), with no statistically significant difference between them ($p = 0.205$), but markedly higher avidity for $HER2^{high}$ targets. In contrast, scFv-based HER2-CAR T cells maintain stronger binding even at low or moderate HER2 density. Together, these kinetic and avidity properties provide a mechanistic basis for the density-gated cytotoxicity of DDMP-based CARs and support their potential to reduce on-target, off-tumor toxicities.

Across constructs, DDMP- and scFv-based CARs exhibited broadly comparable surface expression and transduction efficiency, as quantified by flow cytometry, typically within an approximate two-fold range (**Fig. S6** and **S12**). Except for the avidity and RNA-seq analyses, where CAR-expressing T cells were first isolated and then used for measurement, all other assays used the CAR-positive ratio to calculate the total T cell number required to achieve a defined CAR T cell dose. Although samples with lower CAR-positive ratios contained more untransduced T cells, these cells showed negligible cytotoxicity and cytokine secretion in our assays. It is therefore unlikely that differences in transduction efficiency or expression level are the primary drivers of the phenotypic differences observed between DDMP- and scFv-based CAR T cells.

Interestingly, DDMP-based CAR T cells produced significantly lower levels of pro-inflammatory cytokines IL2, IFNγ, TNFα and GM-CSF than their scFv-based counterparts, a finding supported by both ELISA and RNA-seq data. GSEA revealed that this attenuated cytokine profile was associated with negative enrichment of NF-κB-, NFAT- and KRAS-responsive gene sets in DDMP-based CAR T cells relative to the scFv cohort, with the most consistent differences observed in the NF-κB pathway. This implies that the blunted cytokine output of DDMP-CARs is underpinned by reduced activation of these key signaling pathways. Importantly, while IL2 is required for T cell expansion, its overabundance can cause exhaustion. DDMP-based CAR T cells appear to strike a more favorable balance. This is characterized by moderate IL2 secretion, upregulation of proliferation genes (e.g., MKI67, TOP2A), and the preservation of naïve and memory phenotypic signatures. These traits are collectively associated with sustained antitumor responses.

Traditionally, IFNγ and TNFα production by CAR T cells is viewed as beneficial because these cytokines contribute to tumor cell killing. However, they also activate other immune cells and can amplify inflammatory cascades. Excessive release of IFNγ, TNFα and GM-CSF can ultimately drive CRS, a severe toxicity characterized by systemic inflammation and multi-organ dysfunction. Clinically, CRS risk is primarily assessed by measuring IL6, which is produced mainly by activated macrophages rather than T cells. Our in vitro assays contained only human T cells and tumor cells, and the immunodeficient NCG mice used for in vivo studies possess only defective macrophages. IL6 is therefore not an informative readout in these systems. Instead, we focused on T cell–derived cytokines GM-CSF, IFNγ and TNFα, which drive macrophage proliferation and/or activation and thereby initiate the IL6 amplification loop.[44-47] Notably, GM-CSF inhibition has been shown to reduce CRS and neuroinflammation while enhancing CAR T cell function.[45] Consistent with this biology, the markedly reduced secretion of GM-CSF, IFNγ and TNFα by DDMP-CAR T cells provides a mechanistic basis for lower CRS liability, aligning pathway-level GSEA, cytokine profiles, and functional readouts to support an improved safety profile without loss of antitumor efficacy.

The performance of scFv-based CAR T cells is also shaped by non-binding domains, including spacer, transmembrane, costimulatory and signaling regions. We observed similar architecture-dependence for DDMP-based CARs (**Fig. 1**). For example, constructs incorporating truncated IgG4-Fc variants or a short GSGSGS hexapeptide spacer failed to elicit in vitro cytotoxicity, and variations in spacer, transmembrane

and costimulatory modules modulated cytokine secretion upon exposure to antigen-overexpressing tumor cells. Importantly, we did not observe a simple correlation between in vitro parameters and in vivo efficacy. These findings emphasize that DDMP-CAR performance emerges from an interplay between the binding domain and CAR architecture, and they underscore the need for systematic sequence optimization and in vivo validation. Establishing standardized design principles will facilitate streamlined development and implementation of DDMP-based CAR T therapies against diverse tumor targets.

In conclusion, DDMP-based CAR constructs address key safety limitations of conventional CAR T therapies for solid tumors by combining antigen density-dependent cytotoxicity with attenuated pro-inflammatory cytokine profiles, thereby reducing on-target, off-tumor toxicity and CRS risk while maintaining potent antitumor activity. These results position DDMP-CARs as a promising platform for next-generation CAR T design and highlight DDMPs as a chemically innovative, versatile scaffold for engineering safer yet effective targeted immunotherapies.

Declarations

Ethics approval and consent to participate

All protocols were approved (AECYX202301) by the Institutional Animal Care and Use Committee of the Shenzhen Bay Laboratory (SZBL).

Competing interests

XM, XK, CW and YHT are inventors of a Chinese patent application related to this work.

Acknowledgements

We are grateful to SZBL, Shenzhen Medical Research Fund (D2501002), National Natural Science Foundation of China (22107076), and China Postdoctoral Science Foundation (2024M752146) for the financial support. We thank Prof Shan Tang (University of Science and Technology of China) for helpful discussion, as well as Ms Jingzhe Wang and Ms Maimaiti Ayinazhaer (SZBL) for technical assistance. We appreciate support from the Biomedical Research Core Facilities and Laboratory Animal Center of SZBL, as well as Bio-Tech Center and Animal Experimentation Center of Shenzhen Medical Academy of Research and Translation. During manuscript preparation, the authors used ChatGPT 5.1 for language polishing. All content was subsequently reviewed, revised as necessary, and approved by the authors, who take full responsibility for the final manuscript.

Supporting Information

Supplementary Figures S1−S19; Description of CAR constructs; Experimental procedures on cell culture, PBMC isolation, cell-surface HER2 quantification by flow cytometry, lentivirus packaging, construction of stable cell lines, NFAT activation assay, primary human T cell activation/transduction/expansion, in vitro cytotoxicity and cytokine secretion, RNA-seq analysis, in vivo cytotoxicity, and AlphaFold2 protein structure predictions.

References

(1) June, C. H.; O'Connor, R. S.; Kawalekar, O. U.; Ghassemi, S.; Milone, M. C. CAR T cell immunotherapy for human cancer. *Science* **2018,** *359* (6382), 1361–1365.
(2) Albelda, S. M. CAR T therapy for patients with solid tumours: key lessons to learn and unlearn. *Nat. Rev. Clin. Oncol.* **2024,** *21* (1), 47–66.
(3) Flugel, C. L.; Majzner, R. G.; Krenciute, G.; Dotti, G.; Riddell, S. R.; Wagner, D. L.; Abou-El-Enein, M. Overcoming on-target, off-tumour toxicity of CAR T therapy for solid tumours. *Nat. Rev. Clin. Oncol.* **2023,** *20* (1), 49–62.
(4) Pehlivan, K. C.; Duncan, B. B.; Lee, D. W. CAR-T Cell Therapy for Acute Lymphoblastic Leukemia: Transforming the Treatment of Relapsed and Refractory Disease. *Curr. Hematol. Malig. Rep.* **2018,** *13* (5), 396–406.
(5) Morgan, R. A.; Yang, J. C.; Kitano, M.; Dudley, M. E.; Laurencot, C. M.; Rosenberg, S. A. Case Report of a Serious Adverse Event Following the Administration of T Cells Transduced With a Chimeric Antigen Receptor Recognizing. *Mol. Ther.* **2010,** *18* (4), 843–851.
(6) Sterner, R. C.; Sterner, R. M. CAR-T cell therapy: current limitations and potential strategies. *Blood Cancer J.* **2021,** *11* (4), 69.
(7) Brudno, J. N.; Kochenderfer, J. N. Current understanding and management of CAR T cell-associated toxicities. *Nat. Rev. Clin. Oncol.* **2024,** *21* (7), 501–521.
(8) Caruso, H. G.; Hurton, L. V.; Najjar, A.; Rushworth, D.; Ang, S.; Olivares, S.; Mi, T.; Switzer, K.; Singh, H.; Huls, H.; Lee, D. A.; Heimberger, A. B.; Champlin, R. E.; Cooper, L. J. N. Tuning Sensitivity of CAR to EGFR Density Limits Recognition of Normal Tissue While Maintaining Potent Antitumor Activity. *Cancer Res.* **2015,** *75* (17), 3505–3518.
(9) Liu, X.; Jiang, S.; Fang, C.; Yang, S.; Olalere, D.; Pequignot, E. C.; Cogdill, A. P.; Li, N.; Ramones, M.; Granda, B.; Zhou, L.; Loew, A.; Young, R. M.; June, C. H.; Zhao, Y. Affinity-Tuned ErbB2 or EGFR Chimeric Antigen Receptor T Cells Exhibit an Increased Therapeutic Index against Tumors in Mice. *Cancer Res.* **2015,** *75* (17), 3596–3607.
(10) Arcangeli, S.; Rotiroti, M. C.; Bardelli, M.; Simonelli, L.; Magnani, C. F.; Biondi, A.; Biagi, E.; Tettamanti, S.; Varani, L. Balance of Anti-CD123 Chimeric Antigen Receptor Binding Affinity and Density for the Targeting of Acute Myeloid Leukemia. *Mol. Ther.* **2017,** *25* (8), 1933–1945.
(11) Mao, R.; Kong, W. Q.; He, Y. K. The affinity of antigen-binding domain on the antitumor efficacy of CAR T cells: Moderate is better. *Front. Immunol.* **2022,** *13*, 1032403.
(12) Nishimura, C. D.; Corrigan, D.; Zheng, X. Y.; Galbo, P. M.; Wang, S.; Liu, Y.; Wei, Y.; Suo, L.; Cui, W.; Mercado, N.; Zheng, D.; Zhang, C. C.; Zang, X. TOP CAR with TMIGD2 as a safe and effective costimulatory domain in CAR cells treating human solid tumors. *Sci. Adv.* **2024,** *10* (19), eadk1857.
(13) Yu, S. N.; Yi, M.; Qin, S.; Wu, K. M. Next generation chimeric antigen receptor T cells: safety strategies to overcome toxicity. *Mol. Cancer* **2019,** *18* (1), 125.
(14) Xia, Z.; Jin, Q.; Long, Z.; He, Y.; Liu, F.; Sun, C.; Liao, J.; Wang, C.; Wang, C.; Zheng, J.; Zhao, W.; Zhang, T.; Rich, J. N.; Zhang, Y.; Cao, L.; Xie, Q. Targeting overexpressed antigens in glioblastoma via CAR T cells with computationally designed high-affinity protein binders. *Nat. Biomed. Eng.* **2024,** *8* (12), 1634–1650.
(15) Hebbar, N.; Epperly, R.; Vaidya, A.; Thanekar, U.; Moore, S. E.; Umeda, M.; Ma, J.; Patil, S. L.; Langfitt, D.; Huang, S. J.; Cheng, C.; Klco, J. M.; Gottschalk, S.; Velasquez, M. P. CAR T cells redirected to cell surface GRP78 display robust anti-acute myeloid leukemia activity and do not target hematopoietic progenitor cells. *Nat. Commun.* **2022,** *13* (1), 587.

(16) Wang, D. R.; Starr, R.; Chang, W. C.; Aguilar, B.; Alizadeh, D.; Wright, S. L.; Yang, X.; Brito, A.; Sarkissian, A.; Ostberg, J. R.; Li, L.; Shi, Y. H.; Gutova, M.; Aboody, K.; Badie, B.; Forman, S. J.; Barish, M. E.; Brown, C. E. Chlorotoxin-directed CAR T cells for specific and effective targeting of glioblastoma. *Sci. Transl. Med.* **2020,** *12* (533), eaaw2672.
(17) Choi, J. S.; Joo, S. H. Recent Trends in Cyclic Peptides as Therapeutic Agents and Biochemical Tools. *Biomol. Ther.* **2020,** *28* (1), 18–24.
(18) Rhodes, C. A.; Pei, D. Bicyclic peptides as next-generation therapeutics. *Chem. Eur. J.* **2017,** *23* (52), 12690–12703.
(19) Wu, C. Motif-Directed Oxidative Folding to Design and Discover Multicyclic Peptides for Protein Recognition. *Acc. Chem. Res.* **2025,** *58* (10), 1620–1631.
(20) Liu, H.; Song, L.; Meng, X.; Li, J. L.; Fan, S.; Dong, H.; Wang, X.; Li, M.; Yu, H.; Tsai, Y.-H.; Yin, Y. Y.; Wu, C. Proline-mediated enhancement in evolvability of disulfide-rich peptides for discovering protein binders. *J. Am. Chem. Soc.* **2025,** *147* (28), 24870–24883.
(21) Dong, H. L.; Li, J. J.; Liu, H. T.; Lu, S. M.; Wu, J. J.; Zhang, Y. M.; Yin, Y. Z.; Zhao, Y. B.; Wu, C. L. Design and ribosomal incorporation of noncanonical disulfide-directing motifs for the development of multicyclic peptide libraries. *J. Am. Chem. Soc.* **2022,** *144* (11), 5116–5125.
(22) Zheng, X.; Li, Z.; Gao, W.; Meng, X.; Li, X.; Luk, L. Y. P.; Zhao, Y.; Tsai, Y.-H.; Wu, C. Condensation of 2-((alkylthio)(aryl)methylene)malononitrile with 1,2-aminothiol as a novel bioorthogonal reaction for site-specific protein modification and peptide cyclization. *J. Am. Chem. Soc.* **2020,** *142* (11), 5097–5103.
(23) Xu, C.; Meng, X.; Chai, P.; Liu, H.; Duan, Z.; Tsai, Y.-H.; Wu, C. Directed Evolution of Multicyclic Peptides Using Yeast Display for Sensitive and Selective Fluorescent Analysis of CD28 on the Cell Surface. *Anal. Chem.* **2025,** *97* (7), 4031–4040.
(24) Jonnalagadda, M.; Mardiros, A.; Urak, R.; Wang, X.; Hoffman, L. J.; Bernanke, A.; Chang, W.-C.; Bretzlaff, W.; Starr, R.; Priceman, S.; Ostberg, J. R.; Forman, S. J.; Brown, C. E. Chimeric Antigen Receptors With Mutated IgG4 Fc Spacer Avoid Fc Receptor Binding and Improve T Cell Persistence and Antitumor Efficacy. *Mol. Ther.* **2015,** *23* (4), 757–768.
(25) Lu, S. M.; Fan, S. H.; Xiao, S. L.; Li, J. J.; Zhang, S. L.; Wu, Y. P.; Kong, C. L.; Zhuang, J.; Liu, H. T.; Zhao, Y. B.; Wu, C. L. Disulfide-directed multicyclic peptide libraries for the discovery of peptide ligands and drugs. *J. Am. Chem. Soc.* **2023,** *145* (3), 1964–1972.
(26) Li, N.; Quan, A.; Li, D.; Pan, J. J.; Ren, H.; Hoeltzel, G.; de Val, N.; Ashworth, D.; Ni, W. M.; Zhou, J.; Mackay, S.; Hewitt, S. M.; Cachau, R.; Ho, M. The IgG4 hinge with CD28 transmembrane domain improves VH-based CAR T cells targeting a membrane-distal epitope of GPC1 in pancreatic cancer. *Nat. Commun.* **2023,** *14* (1), 1986.
(27) Chen, H. P.; Wei, F. J.; Yin, M.; Zhao, Q. Y.; Liu, Z. H.; Yu, B. L.; Huang, Z. F. CD27 enhances the killing effect of CAR T cells targeting trophoblast cell surface antigen 2 in the treatment of solid tumors. *Cancer Immunol. Immunother.* **2021,** *70* (7), 2059–2071.
(28) Kennewick, K. T.; Yamaguchi, Y.; Gibson, J.; Gerdts, E. A.; Jeang, B.; Tilakawardane, D.; Murad, J. P.; Chang, W. C.; Wright, S. L.; Thiel, M. S.; Forman, S. J.; Stern, L. A.; Priceman, S. J. Nonsignaling extracellular spacer regulates tumor antigen selectivity of CAR T cells. *Mol. Ther. Oncol.* **2024,** *32* (2), 200789.
(29) Lin, J.; Weiss, A. The tyrosine phosphatase CD148 is excluded from the immunologic synapse and down-regulates prolonged T cell signaling. *J. Cell Biol.* **2003,** *162* (4), 673–682.
(30) Zhang, Y. L.; Patel, R. P.; Kim, K. H.; Cho, H.; Jo, J. C.; Jeong, S. H.; Oh, S. Y.; Choi, Y. S.; Kim, S. H.; Lee, J. H.; Angelos, M.; Guruprasad, P.; Cohen, I.; Ugwuanyi, O.; Lee, Y. G.; Pajarillo, R.; Cho, J. H.; Carturan, A.; Paruzzo, L.; Ghilardi, G.; Wang, M.; Kim, S.; Kim, S. M.; Lee, H. J.; Park, J. H.; Cui, L. G.; Lee, T. B.; Hwang, I. S.; Lee, Y. H.; Lee, Y. J.; Porazzi, P.; Liu, D. F.; Lee, Y.; Kim, J. H.; Lee, J. S.; Yoon,

D. H.; Chung, J.; Ruella, M. Safety and efficacy of a novel anti-CD19 chimeric antigen receptor T cell product targeting a membrane-proximal domain of CD19 with fast on- and off-rates against non-Hodgkin lymphoma: a first-in-human study. *Mol. Cancer* **2023,** *22* (1), 200.
(31) Ferguson, K. M. Structure-based view of epidermal growth factor receptor regulation. *Annu. Rev. Biophys* **2008,** *37*, 353–373.
(32) Jumper, J.; Evans, R.; Pritzel, A.; Green, T.; Figurnov, M.; Ronneberger, O.; Tunyasuvunakool, K.; Bates, R.; Zídek, A.; Potapenko, A.; Bridgland, A.; Meyer, C.; Kohl, S. A. A.; Ballard, A. J.; Cowie, A.; Romera-Paredes, B.; Nikolov, S.; Jain, R.; Adler, J.; Back, T.; Petersen, S.; Reiman, D.; Clancy, E.; Zielinski, M.; Steinegger, M.; Pacholska, M.; Berghammer, T.; Bodenstein, S.; Silver, D.; Vinyals, O.; Senior, A. W.; Kavukcuoglu, K.; Kohli, P.; Hassabis, D. Highly accurate protein structure prediction with AlphaFold. *Nature* **2021,** *596* (7873), 583–589.
(33) Mirdita, M.; Schütze, K.; Moriwaki, Y.; Heo, L.; Ovchinnikov, S.; Steinegger, M. ColabFold: making protein folding accessible to all. *Nat. Methods* **2022,** *19* (6), 679–682.
(34) Barisa, M.; Muller, H. P.; Zappa, E.; Shah, R.; Buhl, J. L.; Draper, B.; Himsworth, C.; Bowers, C.; Munnings-Tomes, S.; Nicolaidou, M.; Morlando, S.; Birley, K.; Leboreiro-Babe, C.; Vitali, A.; Privitera, L.; O'Sullivan, K.; Greppi, A.; Buschhaus, M.; Roman, M. B.; de Blank, S.; van den Ham, F.; van 't Veld, B. R.; Ferry, G.; Fisher, J.; Shome, D.; Nadafi, R.; Ansari, I. H.; Reijmers, R.; Giuliani, S.; Sondel, P.; Donovan, L. K.; Chesler, L.; Jan, M.; Drost, J.; Rios, A. C.; Chester, K.; Wienke, J.; Anderson, J. Functional avidity of anti-B7H3 CAR-T constructs predicts antigen density thresholds for triggering effector function. *Nat. Commun.* **2025,** *16*, 7196.
(35) Dumontet, C.; Reichert, J. M.; Senter, P. D.; Lambert, J. M.; Beck, A. Antibody-drug conjugates come of age in oncology. *Nat. Rev. Drug Discov.* **2023,** *22* (8), 641–661.
(36) Cho, H. S.; Mason, K.; Ramyar, K. X.; Stanley, A. M.; Gabelli, S. B.; Denney, D. W.; Leahy, D. J. Structure of the extracellular region of HER2 alone and in complex with the Herceptin Fab. *Nature* **2003,** *421* (6924), 756–760.
(37) Zhao, Y. B.; Wang, Q. J.; Yang, S. C.; Kochenderfer, J. N.; Zheng, Z. L.; Zhong, X. S.; Sadelain, M.; Eshhar, Z.; Rosenberg, S. A.; Morgan, R. A. A Herceptin-Based Chimeric Antigen Receptor with Modified Signaling Domains Leads to Enhanced Survival of Transduced T Lymphocytes and Antitumor Activity. *J. Immunol.* **2009,** *183* (9), 5563–5574.
(38) Szöor, A.; Tóth, G.; Zsebik, B.; Szabó, V.; Eshhar, Z.; Abken, H.; Vereb, G. Trastuzumab derived HER2-specific CARs for the treatment of trastuzumab-resistant breast cancer: CAR T cells penetrate and eradicate tumors that are not accessible to antibodies. *Cancer Lett.* **2020,** *484*, 1–8.
(39) Hernandez-Lopez, R. A.; Yu, W.; Cabral, K. A.; Creasey, O. A.; Pazmino, M. D. L.; Tonai, Y.; De Guzman, A.; Makela, A.; Saksela, K.; Gartner, Z. J.; Lim, W. A. T cell circuits that sense antigen density with an ultrasensitive threshold. *Science* **2021,** *371* (6534), 1166–1171.
(40) Vitanza, N. A.; Johnson, A. J.; Wilson, A. L.; Brown, C.; Yokoyama, J. K.; Künkele, A.; Chang, C. A.; Rawlings-Rhea, S.; Huang, W. J.; Seidel, K.; Albert, C. M.; Pinto, N.; Gust, J.; Finn, L. S.; Ojemann, J. G.; Wright, J.; Orentas, R. J.; Baldwin, M.; Gardner, R. A.; Jensen, M. C.; Park, J. R. Locoregional infusion of HER2-specific CAR T cells in children and young adults with recurrent or refractory CNS tumors: an interim analysis. *Nat. Med.* **2021,** *27* (9), 1544–1552.
(41) Ma, Q. Z.; He, X.; Zhang, B. X.; Guo, F. C.; Ou, X. J.; Yang, Q. Y.; Shu, P.; Chen, Y.; Li, K.; Gao, G.; Zhu, Y. J.; Qin, D. Y.; Tang, J.; Li, X. Y.; Jing, M.; Zhao, J.; Mo, Z. M.; Liu, N.; Zeng, Y.; Zhou, K. X.; Feng, M. Y.; Liao, W. T.; Lei, W. T.; Li, Q.; Li, D.; Wang, Y. S. A PD-L1-targeting chimeric switch receptor enhances efficacy of CAR-T cell for pleural and peritoneal metastasis. *Signal Transduct. Target Ther.* **2022,** *7* (1), 380.
(42) Silman, I.; Zwaagstra, J. C.; Sulea, T.; Baardsnes, J.; Radinovic, S.; Cepero-Donates, Y.; Robert, A.;

O'Connor-McCourt, M. D.; Tikhomirov, I. A.; Jaramillo, M. L. Binding and functional profiling of antibody mutants guides selection of optimal candidates as antibody drug conjugates. *PLoS One* **2019,** *14* (12), e0226593.
(43) Chen, Y.; Ye, Z.; Cho, W. C.; Zhang, D. X. Cell avidity in CAR-T cell therapy. *Expert Rev. Mol. Diagn.* **2025,** *25* (11), 737–740.
(44) Lee, K. M. C.; Achuthan, A. A.; Hamilton, J. A. GM-CSF: A Promising Target in Inflammation and Autoimmunity. *ImmunoTargets and Therapy* **2020,** *9*, 225–240.
(45) Sterner, R. M.; Sakemura, R.; Cox, M. J.; Yang, N.; Khadka, R. H.; Forsman, C. L.; Hansen, M. J.; Jin, F.; Ayasoufi, K.; Hefazi, M.; Schick, K. J.; Walters, D. K.; Ahmed, O.; Chappell, D.; Sahmoud, T.; Durrant, C.; Nevala, W. K.; Patnaik, M. M.; Pease, L. R.; Hedin, K. E.; Kay, N. E.; Johnson, A. J.; Kenderian, S. S. GM-CSF inhibition reduces cytokine release syndrome and neuroinflammation but enhances CAR-T cell function in xenografts. *Blood* **2019,** *133* (7), 697–709.
(46) Salim, T.; Sershen, C. L.; May, E. E. Investigating the Role of TNF-α and IFN-γ Activation on the Dynamics of iNOS Gene Expression in LPS Stimulated Macrophages. *PLoS One* **2016,** *11* (6), e0153289.
(47) Zhang, F.; Mears, J. R.; Shakib, L.; Beynor, J. I.; Shanaj, S.; Korsunsky, I.; Nathan, A.; Accelerating Medicines Partnership Rheumatoid, A.; Systemic Lupus Erythematosus, C.; Donlin, L. T.; Raychaudhuri, S. IFN-γ and TNF-α drive a CXCL10+ CCL2+ macrophage phenotype expanded in severe COVID-19 lungs and inflammatory diseases with tissue inflammation. *Genome Med.* **2021,** *13* (1), 64.
(48) Liu, X.; Ma, L.; Li, J.; Sun, L.; Yang, Y.; Liu, T.; Xing, D.; Yan, S.; Zhang, M. Trop2-targeted therapies in solid tumors: advances and future directions. *Theranostics* **2024,** *14* (9), 3674–3692.
(49) Zhang, X.; Xiao, H.; Na, F.; Sun, J.; Guan, Q.; Liu, R.; Cai, L.; Li, H.; Zhao, M. Evolution of TROP2: Biological insights and clinical applications. *Eur. J. Med. Chem.* **2025,** *296*, 117863.
(50) Gomes-Silva, D.; Mukherjee, M.; Srinivasan, M.; Krenciute, G.; Dakhova, O.; Zheng, Y.; Cabral, J. M. S.; Rooney, C. M.; Orange, J. S.; Brenner, M. K.; Mamonkin, M. Tonic 4-1BB Costimulation in Chimeric Antigen Receptors Impedes T Cell Survival and Is Vector-Dependent. *Cell Rep.* **2017,** *21* (1), 17–26.
(51) Long, A. H.; Haso, W. M.; Shern, J. F.; Wanhainen, K. M.; Murgai, M.; Ingaramo, M.; Smith, J. P.; Walker, A. J.; Kohler, M. E.; Venkateshwara, V. R.; Kaplan, R. N.; Patterson, G. H.; Fry, T. J.; Orentas, R. J.; Mackall, C. L. 4-1BB costimulation ameliorates T cell exhaustion induced by tonic signaling of chimeric antigen receptors. *Nat. Med.* **2015,** *21* (6), 581–90.
(52) Larson, R. C.; Maus, M. V. Recent advances and discoveries in the mechanisms and functions of CAR T cells. *Nat. Rev. Cancer* **2021,** *21* (3), 145–161.
(53) Wu, Y. P.; Fan, S. H.; Dong, M.; Li, J. J.; Kong, C. L.; Zhuang, J.; Meng, X. T.; Lu, S. M.; Zhao, Y. B.; Wu, C. L. Structure-guided design of CPPC-paired disulfide-rich peptide libraries for ligand and drug discovery. *Chem. Sci.* **2022,** *13* (26), 7780–7789.
(54) Li, J.; Liu, H.; Xiao, S.; Fan, S.; Cheng, X.; Wu, C. De Novo Discovery of Cysteine Frameworks for Developing Multicyclic Peptide Libraries for Ligand Discovery. *J. Am. Chem. Soc.* **2023,** *145* (51), 28264–28275.
(55) Wu, C.; Liu, H.; Dong, M. High affinity Trop2 targeting multi-cyclic peptide molecular framework. 2022.
(56) Rossi, E. A.; Rossi, D. L.; Cardillo, T. M.; Chang, C. H.; Goldenberg, D. M. Redirected T-cell killing of solid cancers targeted with an anti-CD3/Trop-2-bispecific antibody is enhanced in combination with interferon-alpha. *Mol. Cancer Ther.* **2014,** *13* (10), 2341–51.